Journal of Cancer Epidemiology and Prevention

Open access Research Article

Characterization of the Solitary Pulmonary Nodule (NPS): Comparison of Positron Emission Tomography-Computer Tomography (PET-CT) and MRI in Diffusion Weighted Imaging/Apparent Diffusion Coefficient (DWI/ADC) sequences: A Pilot Study

Gianluigi Sergiacomi[1], Carlotta Rellini[1*], Adriano Lacchè[2], Flavia Rufi[1], Francesca Montesanto[1], Federica Ricciardi[1], Eugenio Pompeo[3], Paola Rogliani[4], Roberto Floris[1], Orazio Schillaci[1]

[1]Department of Diagnostic Imaging and Interventional Radiology, University Rome Tor Vergata, Italy
[2]Department of Dermopathic Institute of the Immaculate IRCSS of Rome, Italy
[3]Department of Biomedicine and Prevention, University of Rome Tor Vergata, Italy
[4]Department of Experimental Medicine, University of Rome Tor Vergata, Italy

ABSTRACT

Objectives: This study proposes to present Magnetic resonance imaging (MRI) with Diffusion Weighted Imaging (DWI) sequences and Apparent Diffusion Coefficient (ADC) maps as an innovative and safe method for pulmonary nodule characterization, comparing it with PET-CT with 18FDG and prove that MRI is promising as an alternative technique in distinguishing benign from malignant solitary pulmonary nodules, without presenting significant differences to predict the malignancy of pulmonary nodules.

Results: comparing the two methods in the optimal cut-offs for our population, MRI demonstrates higher sensitivity than PET-CT (84.6% vs. 69.2%) against equal specificity (83.3%).

Conclusion: DWI/ADC sequences have been shown to be effective in distinguishing benign from malignant solitary pulmonary nodules. Comparison of MRI and PET-CT showed no statistically significant differences in the ability to predict the malignancy of pulmonary nodules.

Abbreviations and acronyms: Solitary Pulmonary Nodules (NPS), Single-Shot Echo Planar Imaging (SS EPI), 2-deoxy-2-fluoro-D-glucose (18FDG)

Keywords: Magnetic resonance imaging; Solitary pulmonary nodule; Malignant pulmonary nodule; Diffusion Weighted Imaging, ADC maps, PET-TC

Received:	02-May-2023	**Manuscript No:**	IPJCEP-23-16340
Editor assigned:	04-May-2023	**PreQC No:**	IPJCEP-23-16340(PQ)
Reviewed:	18-May-2023	**QC No:**	IPJCEP-23-16340
Revised:	23-May-2023	**Manuscript No:**	IPJCEP-23-16340 (R)
Published:	30-May-2023	**DOI:**	10.36648/IPJCEP.23.08.12

Corresponding author Carlotta Rellini, Department of Diagnostic Imaging and Interventional Radiology, University Rome Tor Vergata, Italy, E-mail: carlottarellini@gmail.com

Citation Sergiacomi G, Rellini C, Lacchè A, Rufi F, Montesanto F, et al. (2023) Characterization of the Solitary Pulmonary Nodule (NPS): Comparison of Positron Emission Tomography-Computer Tomography (PET-CT) and MRI in Diffusion Weighted Imaging/Apparent Diffusion Coefficient (DWI/ADC) sequences: A Pilot Study. J Cancer Epidemiol Prev. 8:12.

INTRODUCTION

The solitary pulmonary nodule is defined radio-logically as focal, roughly circular, not always well-circumscribed lung opacity with a maximum diameter of less than 3 cm and surrounded by normal lung parenchyma or in contact with the pleura. Nodules may be single or multiple and can be found in the lung without other abnormalities such as lymphadenopathy or pleural disease [1,2]. A pulmonary nodule is an occasional finding on imaging studies unrelated to the respiratory system in 0.09%-0.2% of cases [3] and a frequent finding of all chest radiographs computed tomography [4,5]. The presence of a solitary pulmonary nodule opens the path to several different diagnoses. Recent review shows around 10%-20% of nodules are malignant [6]. Diagnostic imaging must quickly recognize the nature of the nodule to avoid non-proportional treatments and procedures. PET-CT with FDG-18 is now the gold-standard; magnetic resonance imaging (MRI) is starting to take its first steps with promising results. The radiological assessment of the pulmonary nodule is carried out using the guidelines of the Fleischner Society and Lung-RADS, produced by the American College of Radiology. The main radiological indicators of malignancy are morphology, size, location, number of nodules and doubling time. Nodules can be divided into solid, subsolid and ground-glass. [7].

Solid and sub-solid nodules have a higher risk of malignant transformation (6.6% to 22.2%) than ground-glass nodules (1.3% to 1.9%) [8]. The size and volume of the nodule must then be assessed; a solid component greater than 5 mm depicts an increased likelihood of local invasion [9,10]. A recent trial showed that nodules >10 mm or >300 mm^3 have a 9.7%=-16.9% probability of malignant transformation at 2 years. Patients with solid nodules <5 mm or <100 mm^3 have the same probability of developing neoplastic pathology as the population in which no nodules were found at screening (**Figure 1**). Sub-solid nodules have a more indolent growth with rare and distant neoplastic transformation, [11] and lesions larger than 10 mm in diameter have shown a more aggressive course [12]. The likelihood of malignancy also increases in the presence of spiculated margins, upper lobe localization (doubled risk compared to other sites) [13], a smaller number of nodules (patients with 5 or more nodules are less likely to develop neoplastic disease than patients with less than 5 nodules) [14], and a doubling time of 100-400 days [15].

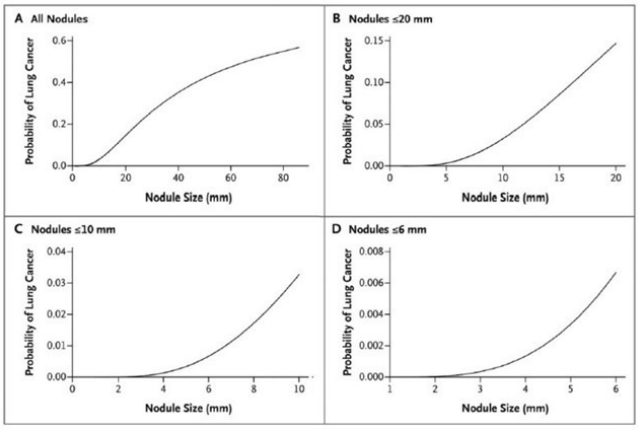

Figure1: Correlation between size and malignancy in solitary pulmonary nodule. A) All sizes; B) less than or equal to 20 mm; C) less than or equal to 10 mm; D) less than or equal to 6 mm.

After solitary pulmonary nodule detection, 18FDG-PET remains the first choice in characterization [16], with a sensitivity and specificity of approximately 95% and 82%. The accuracy of PET is also affected by nodule composition, as it is less sensitive and specific in ground-glass nodules, the detection rate of PET-CT for malignant lesions is about 62.9%, with a positive rate of 82.9% and a false positive rate of 58.3% [17]. Magnetic resonance imaging was for years considered inapplicable in the study of lung neoplasms because of the low proton density in ventilated healthy lung tissue and of image distortion generated by the air-parenchyma interface and respiratory and cardiac motion [18]. The introduction of single-shot Echo Planar Imaging sequences that allow much faster and less motion-sensitive acquisitions, of the possibility to synchronize acquisitions with breath phases or heart rate, of functional imaging techniques such as diffusion (DWI) and dynamic contrast-enhanced studies (DCE-MRI), have greatly changed the fields of applicability of this technique [19].

Objectives

The study aims to relate the data obtained in DWI with the results of PET-CT and histology by comparing the ability of the two methods in recognizing nodules and characterizing them. Our sample size is 50 nodules out of 48 patients.

MATERIALS AND METHODS

We chose to conduct a prospective study to select newfound nodules without histological diagnosis. Patients with no absolute or relative contraindications to MRI with a lung nodule <30 mm on chest HRCT were included. Of our 48 patients, 37 presented for an outpatient check-up prescribed by the general practitioner for cough or generic indication and 11 patients were hospitalized for other non-oncological causes, so nodules were found during HRCT of the chest performed as a pre-operative check or in the suspicion of inflammatory diseases (excluded by HRCT). Patients with radiological evidence of pneumonia, patients with previous lung surgery or with metallic thoracic devices, patients with contraindications to MRI, patients at high risk of biopsy, for nodule placement or medical condition, were excluded. Patients underwent PET-CT low dose with 18FDG within two weeks before or after the MRI examination. The examinations were performed with a high-field device (3T) with sequences

- T2w axial and coronal
- Dual FFE
- DWI with b0, b500, b800 and b1000 and ADC maps

The diffusivity coefficient was calculated by placing the ROI (region of interest) on the ADC map at the site of the solid component, avoiding necrotic areas and allowing for no underestimation of tumor heterogeneity (**Figure 2**). Statistical analysis was conducted using MedCalc Statistical Software version 19.3.1 (MedCalc Software; https://www.medcalc.org; 2016). Lesions with SUV max and ADC mean values above the cut-off were considered positive while those below as negative for PET-CT and DWI, respectively. ROC curves were compared using z-tests. Exams were well tolerated by all patients. The average duration of the MRI examinations was 17.1 ± 2.1 minutes. No examina-

tion was prematurely interrupted, and all patients easily understood and applied the instructions given automatically by the machine.

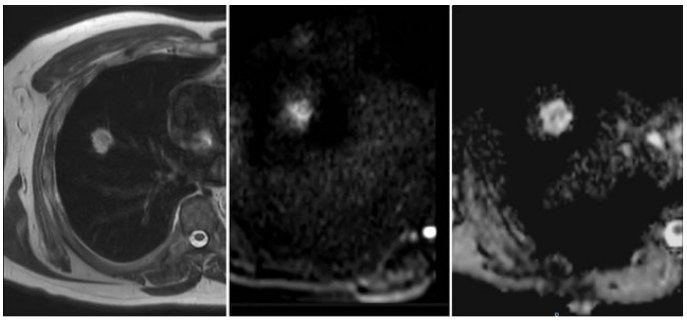

Figure 2: MRI images in different sequences in a patient with a 25-mm nodule. Left. T2-weighted sequence. Middle. DWI-weighted sequence. Right. Image reconstruction in ADC. (DWI: Diffusion Weighted Imaging, ADC: Apparent Diffusion Coefficient).

RESULTS

In all patients, the diagnosis was made by histological examination, obtained by Awake VATS or CT-guided biopsy. Histological examination of the 26 high-risk nodules revealed 24 malignant and 2 benign nodules (one chronic inflammation and one granuloma), while examination of the 24 low-risk nodules confirmed 23 as benign and 1 nodule as neoplastic (acinar variant adenocarcinoma). Among the 24 malignant nodules, 22 primary lung tumors (16 adenocarcinomas and 6 squamous cell tumors), 1 marginal B-cell lymphoma and 1 solitary malignant fibrous tumor of the pleura were found. Among the 24 benign nodules, 10 hamartomas, 8 granulomas and 6 chronic inflammatory processes with pictures of organizing pneumonia (BOOP/COP) were identified. The mean size of the benign nodules was 16.0 ± 7.45 mm^3, whereas the mean size of the malignant nodules was 21.7 ± 7.27 mm^3, and the difference between the two groups was not statistically significant (p=0.007). The mean volume of the benign nodules was 3478.2 ± 4654.7 mm^3, while in the malignant 9110.3 ± 5351.6 mm^3. The differences between the two populations were found to be non-significant (p=0.010). Threshold values for the two imaging techniques were calculated using ROC curve. From the ROC curves of the generated ADC maps (B0: 0-500, 0-800 and 0-1000), values lower than 1.14 x 10^{-3} mm^2/s, 1.07 x 10^{-3} mm^2/s and 1.20 x 10^{-3} mm^2/s, respectively, were identified as the optimal cutoff for the diagnosis of malignancy in DWI. From the ROC curve for SUV max, a value of SUV max>4 was identified as the optimal cutoff for the diagnosis of malignancy in PET-CT. In MRI, the values obtained with the gradient b 0-800 were chosen as the quantitative benchmark for DWI considering the relationship between the higher value of b and the quality of the images obtained (**Figure 3**). The mean ADC mean value found in benign nodules was 1.57 ± 0.56 x 10^{-3} mm^2/s, while the value in malignant nodules was 0.89 ± 0.19 x 10^{-3} mm^2/s. The ADC mean values for malignant nodules were significantly lower than the ADC mean values found in benign nodules (p=0.002). When the cutoff of 1.07 x 10^{-3} mm^2/s was applied, the sensitivity and specificity obtained were 84.6% and 83.3%, respectively. No significant difference was found between the ADC mean values in the different histo-types of the malignant nodules. The values of ADC mean and SUV max show a significant inverse correlation according to Spearman's test (rho=-0.731) (p<0.001). The analysis of the ROC curves obtained from the ADC mean values calculated for b=0 and b=800 and SUV max showed an AUC of 0.875 and an AUC of 0,859 respectively. Z-test demonstrated the absence of statistical significance in the distinction between the two curves (p=0.811). Graphical comparison of the two curves is shown in the **Figure 4**. When comparing the two methods in the optimal cutoff for our population, MRI demonstrates a higher sensitivity than PET-CT (84.6% vs. 69.2%) against an equal specificity (83.3%).

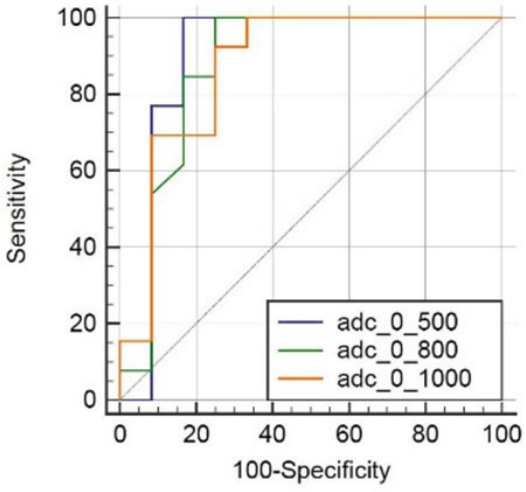

Pairwise comparison of ROC curves

adc_0_500 ~ adc_0_800	
Difference between areas	0,0224
Standard Error [a]	0,0471
95% Confidence Interval	-0,0699 to 0,115
z statistic	0,476
Significance level	P = 0,6338
adc_0_500 ~ adc_0_1000	
Difference between areas	0,0256
Standard Error [a]	0,0516
95% Confidence Interval	-0,0754 to 0,127
z statistic	0,497
Significance level	P = 0,6191
adc_0_800 ~ adc_0_1000	
Difference between areas	0,00321
Standard Error [a]	0,0263
95% Confidence Interval	-0,0483 to 0,0547
z statistic	0,122
Significance level	P = 0,9029

[a] DeLong et al., 1988

Figure 3: ROC curve drawn on ADC values in the three different gradients b 0-500, b 0-800 and b 0-1000. Bottom, pairwise comparison showing no statistically significant differences between the AUCs of the three ROCs).

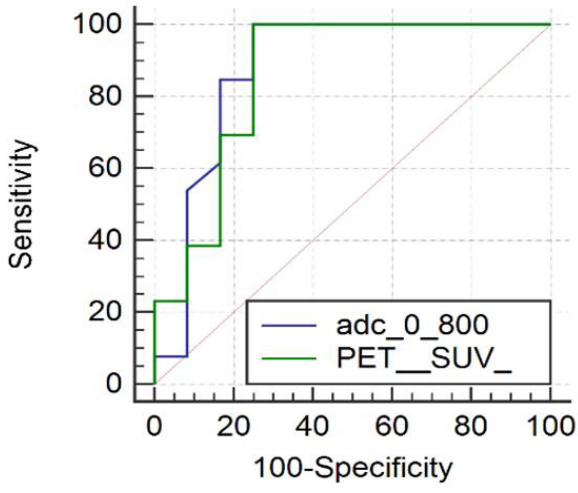

Figure 4: Comparison of ROC curves drawn with ADCmean (b 0-800) and SUVmax values.

DISCUSSION

The main limitation of our study is the small number of nodules analyzed. Larger multicenter studies with very large patient samples will certainly be needed in the future to confirm the hypothesis that MRI is a valid alternative to PET-CT with 18FDG. Another limitation is represented by the variety of malignant pathology present in our sample, which does not allow, in relation to the scarcity of the sample, to standardize the ADC values for one or the other malignant type. We can confirm that our goal was only to discriminate malignant formations from benign ones, and further studies are also needed in this direction.

In our study, 8 of the 50 nodules examined had a diameter below 10 mm with a nadir at 7 mm. PET correctly estimated the risk of malignancy in 4/8 nodules while MRI in 6/8 nodules. Considering the lack of definite data in the literature and the small size of our sample, further targeted studies needed to investigate the applicability of MRI DWI/ADC sequences in sub-centimetric nodules. The prevalence of sub-solid nodules as well as their biological significance is not widely elucidated. Screening data show an incidence in at-risk populations of up to 15.9% ground-glass nodules and up to 4.3% partially solid nodules [20]. In our study, 6 sub-solid nodules were included (**Figure 5**), excluding nodules with only ground glass component; MRI correctly characterized the nodules in 4/6 cases, while PET-CT in 2/6 cases. Further studies are needed. In our study, the two techniques compared in all 50 nodules **Figure 6** showed no significant differences. MRI showed a sensitivity of 84.6% compared to 69.2% for PET-CT, while the specificity was 83.3% for both techniques.

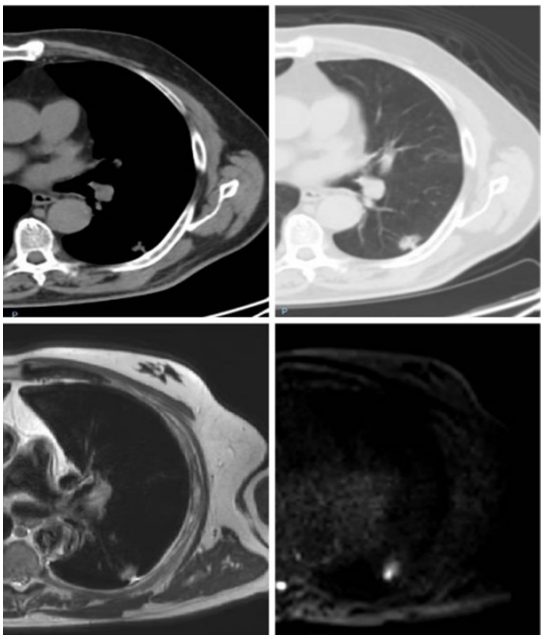

Figure 5: MRI application in a sub-solid nodule. The other left. Chest CT scan in parenchymal window. Top right. CT thorax in mediastinal window (soft tissue). Bottom left. MRI in T2-weighted sequences. Bottom right. MRI in DWI sequences.

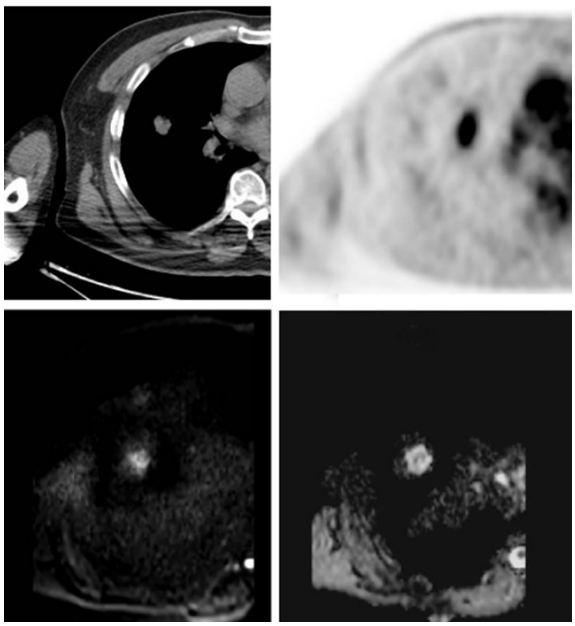

Figure 6: MRI and PET-CT comparison in a patient with a 25-mm malignant nodule. Top left. CT scan of the chest. Top right. WB QClear in PET. Bottom left. DWI MRI. Bottom right. ADC in MRI.

The smallness of our sample and the lack of standardization of MRI values led us to contextualize our study results in comparison with other studies [21], evaluating the discriminative ability of DWI to detect benign and malignant lesions and comparing DWI with PET-TC. Therefore, we included two kinds of studies aimed at predicting lung nodule malignancy [22-24] and studies comparing DWI with PET-CT [25]. The mean sensitivity value obtained in these studies [26-28] was 89.6% (73.3%-100%) while the mean specificity was 79.9% (36%-100%). Our study is in line with the average sensitivity and specificity values reported in the literature with a value of 84.6% and 83.3%. In most cases the two methods are equivalent, although in one study Mori et al describes a better ability of MRI to discriminate active inflammatory lesions from neoplastic pathology. In some of the reported studies [29], the correlation between ADC and SUVmax and the stage, degree of invasiveness or cellularity of the lesions is investigated. Among these prognostic factors, only the correlation between lesion cellularity and ADC is well documented [30]. These considerations are beyond the scope of our study, but the prognostic significance of ADC and its possible applications showed promising results [31]. Characterization of the pulmonary nodule, as we have seen, includes numerous diagnostic examinations with increasing invasiveness and cost. Our study, contextualized with other recent works in the literature, demonstrates, albeit on a small sample, the effectiveness of magnetic resonance imaging in the characterization of pulmonary nodules [32-34].

CONCLUSION

PET scan costs € 850 while a PET-CT scan is about € 1071.65. The cost of a chest MRI is 115.8 € and increases to 181.28 € with contrast injection. Chest MRI costs about seven times less than PET and more than nine times less than PET-CT. MRI is proposed as a safe radiation-free examination in the second-level characterization of pulmonary nodule. However, the limited availability of the technique and low number of publications reflected in the lack of standardization and great heterogeneity in the parameters used to perform exams. However, MRI and the application of DWI/ADC sequences in the pulmonary nodule have several limitations, such as the poor reproducibility of results with different machines and the presence of various contraindications to perform the examination linked to the use of magnetic fields and patient characteristics.

The limited number of patients of our sample did not allow us to establish a correlation between ADC and histology nor the characterization within the same histo-type of neoplasms with different degrees of malignancy. Furthermore, other ADC values such as ADC minimum or the ratio of ADC calculated in the necrotic areas to the wall (necrosis/wall ratio) could not be taken in the study as has been done with promising results in other studies. In addition, it might be promising to evaluate the behavior of lung nodules even after the administration of intravenous paramagnetic mdc, but it was not possible because it was a pilot study. This preliminary study has demonstrated the ability of MRI DWI sequences, evaluated with ADC maps, to distinguish benign from malignant solitary pulmonary nodules. Comparison of this technique with PET-CT showed no statistically significant differences to predict the malignancy of pulmonary nodules. The results of our study were affected by a reduced sample size. We can recognize that the advantages of this technique in terms of biological risks and social and economic costs are considerable, and any doubts regarding the acceptance of the examination of patients and the presence of artefacts due to the intrinsic characteristics of the lung parenchyma were not significantly reflected in our study. Further studies with larger populations and standardized parameters are needed to establish the relevance of this technique in the clinical setting.

CONFLICT OF INTEREST

There are no conflicts of interest.

ACKNOWLEDGEMENT

None.

REFERENCES

1. Callister MEJ, Baldwin DR, Akram AR, Barnard S, Cane P, et al. (2015) British thoracic society guidelines for the investigation and management of pulmonary nodules. Thorax. 70: ii1–ii54.
2. Khan AN, Al-Jahdali HH, Irion KL, Arabi M, Koteyar SS (2011) Solitary pulmonary nodule: A diagnostic algorithm in the light of current imaging technique. Avicenna J Med. 1(2): 39–51.
3. Hall WB, Truitt SG, Scheunemann LP, Shah SA, Rivera MP, et al. (2009) The prevalence of clinically relevant incidental findings on chest computed tomographic angiograms ordered to diagnose pulmonary embolism. ArchInternMed. 169: 1961–1965.
4. Song JH, Beland MD, Mayo-Smith WW (2012) Incidental clinically important extraurinary findings at MDCT urography for hematuria evaluation: Prevalence in 1209 consecutive examinations. Am J Roentgenol. 199: 616–622.
5. Van Riel SJ, Sánchez CI, Bankier AA, Naidich DP, Verschakelen J, et al. (2015) Observer variability for classification of pulmonary nodules on low-dose CT images and its effect on nodule management. Radiology. 277:863–871.
6. Tammemagi MC, Schmidt H, Martel S, McWilliams A, Goffin JR, et al. (2017) Participant selection for lung cancer screening by risk modelling: A single-arm, prospective study. Lancet Oncol. 18 :1523-1531.
7. McWilliams A, Tammemagi MC, Mayo JR, Liu G, Soghrati K, et al. (2013) Probability of cancer in pulmonary nodules detected on first screening CT. N Engl J Med. 369: 910–919.
8. Saji H, Matsubayashi J, Akata S, Shimada Y, Kato Y, et al. (2015) Correlation between whole tumor size and solid component size on high-resolution computed tomography in the prediction of the degree of pathologic malignancy and the prognostic outcome in primary lung adenocarcinoma. ActaRadiol. 56:1187–1195.
9. Horeweg N, van Rosmalen J, Heuvelmans MA, M vander Aalst C, Vliegenthart R, et al. (2014) Lung cancer probability in patients with CT-detected pulmonary nodules: A prespecified analysis of data from the NELSON trial of low-dose CT screening. Lancet Oncol. 15: 1332–1341.

10. Yankelevitz DF, Yip R, Smith JP, Liang M, Liu Y, et al. (2015) CT screening for lung cancer: Nonsolid nodules in baseline and annual repeat rounds. Radiology. 277: 555–564.

11. Silva M, Bankier AA, Centra F (2015) Longitudinal evolution of incidentally detected solitarypure ground-glass nodules on CT: Relation to clinical metrics. DiagnIntervRadiol. 21: 385–390.

12. Peters R, Heuvelmans MA, Vliegenthart R, Van Ooijen PM, De Bock GH, et al. (2015) Prevalence of pulmonary multi-nodularity in CT lung cancer screening and lung cancer probability. In: Radiological society of North America scientific assembly and annual meeting program. Oak-Brook, Ill: Radiological Society of North America.

13. Hasegawa M, Sone S, Takashima S, Li F, Yang ZG, et al. (2000) Growth rate of small lung cancers detected on mass CT screening. Br J Radiol. 73: 1252–1259.

14. Cardiff (UK) (2011) The diagnosis and treatment of lung cancer (Update). National Institute for Health and Clinical Excellence: Guidance.

15. Cronin P, Dwamena BA, Kelly AM (2008) Solitary pulmonary nodules: Meta-analytic comparison of cross-sectional imaging modalities for diagnosis of malignancy. Radiology. 246: 772–82.

16. Kauczor HU, Ley S (2010) Thoracic magnetic resonance imaging 1985 to 2010. J ThoracImaging.25: 34-38.

17. Turner R, Le Bihan D, Maier J, Vavrek R, Hedges LK, et al. (1990) Echo-planar imaging of intravoxel incoherent motion. Radiology. 177: 407-14.

18. Luna A, Sánchez-Gonzalez J, Caro P (2011) Diffusion-weighted imaging of the chest. MagnResonImagingClin N Am. 19: 69–94.

19. Matoba M, Tonami H, Kondou T, Yokota H, Higashi K, et al. (2007) Lung carcinoma: Diffusion-weighted MR imaging-preliminary evaluation with apparent diffusion coefficient. Radiology. 243: 570–577.

20. Can TS, Uzan G (2019) Comparison of the diagnostic accuracy of diffusion-weighted magnetic resonance imaging and positron emission tomography/computed tomography in pulmonary nodules: A prospective study. Pol J Radiol. 84: e498–e503.

21. Yuan M, Zhong Y, Zhang YD, Fu Yu T, Li H, et al. (2017) Volumetric analysis of intravoxel incoherent motion imaging for assessment of solitary pulmonary lesions. Acta Radiologica 58:1448–1456.

22. Komori T, Narabayashi I, Matsumura K, Matsuki M, Akagi H, et al. (2007) 2-[Fluorine-18]-fluoro-2-deoxy-d- glucose positron emission tomography/computed tomography versus whole-body diffusion- weighted MRI for detection of malignant lesions: Initial experience. Annals of Nuclear Medicine. 21: 209–215.

23. Mori T, Nomori H, Ikeda K, Kawanaka K, Shiraishi S, et al. (2008) Diffusion-weighted magnetic resonance imaging for diagnosing malignant pulmonary nodules/masses: Comparison with positron emission tomography. J ThoracOncol 3: 358–64.

24. Kanauchi N, Oizumi H, Honma T, Kato H, Makoto Endo M, et al. (2009) Role of diffusion-weighted magnetic resonance imaging for predicting of tumor invasiveness for clinical stage IA non-small cell lung cancer. Eur J CardiothoracSurg. 35: 706–711.

25. Zhang J, Cui LB, Tang X, Ren XL, Shi JR, et al. (2014) DWMRI at 3.0 T versus FDG PET/CT for detection of malignant pulmonary tumors. Int J Cancer. 134: 606–611.

26. Usuda K, Funasaki A, Sekimura A, Motono N, Matoba M, et al. (2018) FDG-PET/CT and diffusion-weighted imaging for resected lung cancer: Correlation of maximum standardized uptake value and apparent diffusion coefficient value with prognostic factors. MedOncol. 35: 66.

27. De Hoop B, van Ginneken B, Gietema H, Prokop M (2012) Pulmonary perifissural nodules on CT scans:Rapid growth is not a predictor of malignancy. Radiology. 265: 611–16.

28. Zurstrassen CE, Tyng CJ, Guimarães MD, Barbosa P, Pinto C, et al. (2020) Functional and metabolic imaging intransthoracic biopsies guided by computed tomography. EurRadiol. 30: 2041-2048.

29. Karaman A, Durur-Subasi I, Alper F (2017) Is it better to include necrosis in apparent diffusion coefficient (ADC) measurements? The necrosis/wall ADC ratio to differentiate malignant and benign necrotic lung lesions: Preliminary results. Journal of MagneticResonanceImaging. 46:1001–1006.

30. Ohba Y, Nomori H, Mori T, Ikeda K, Shibata H, et al. (2009) Is diffusion-weighted magnetic resonance imaging superior topositron emission tomography with fludeoxyglucose F 18 in imaging non-small cell lungcancer? J ThoracCardiovascSurg. 138: 439–445.

31. Tsuchida T, Morikawa M, Demura Y, Umeda Y, Okazawa H, et al. (2013) Imaging the early response to chemotherapy in advanced lung cancer with diffusion-weighted magnetic resonance imaging compared to fluorine-18 fluorodeoxyglucose positron emission tomography and computed tomography. J MagnResonImaging; 38: 80-88.

32. Ohno Y, Koyama H, Yoshikawa T, Matsumoto K, Aoyama N, et al. Diffusion-weighted MRI versus 18F- FDG PET/CT: Performance as predictors of tumor treatment response and patient survival in patients with non-small cell lung cancer receiving chemoradiotherapy. AJR Am J Roentgenol2012; 198: 75- 82.

33. Chin Wan Koo, Aiming (2019) Can MRI contribute to pulmonarynoduleanalysis?. JMagnResonImaging. 49(7):e256-e264.

34. Ohno Y, Kauczor HU, Hatabu H, Seo JB, Jr van Beek E, et al. (2020) MRI for solitarypulmonarynodule and mass assessment: Current state of the art. J MagnResonImaging.